Equation of State and Material Properties of Dense QCD Matter from (2+1)-flavor Lattice QCD

Jishnu Goswami

HotQCD collaboration

Critical points in the QCD phase diagram

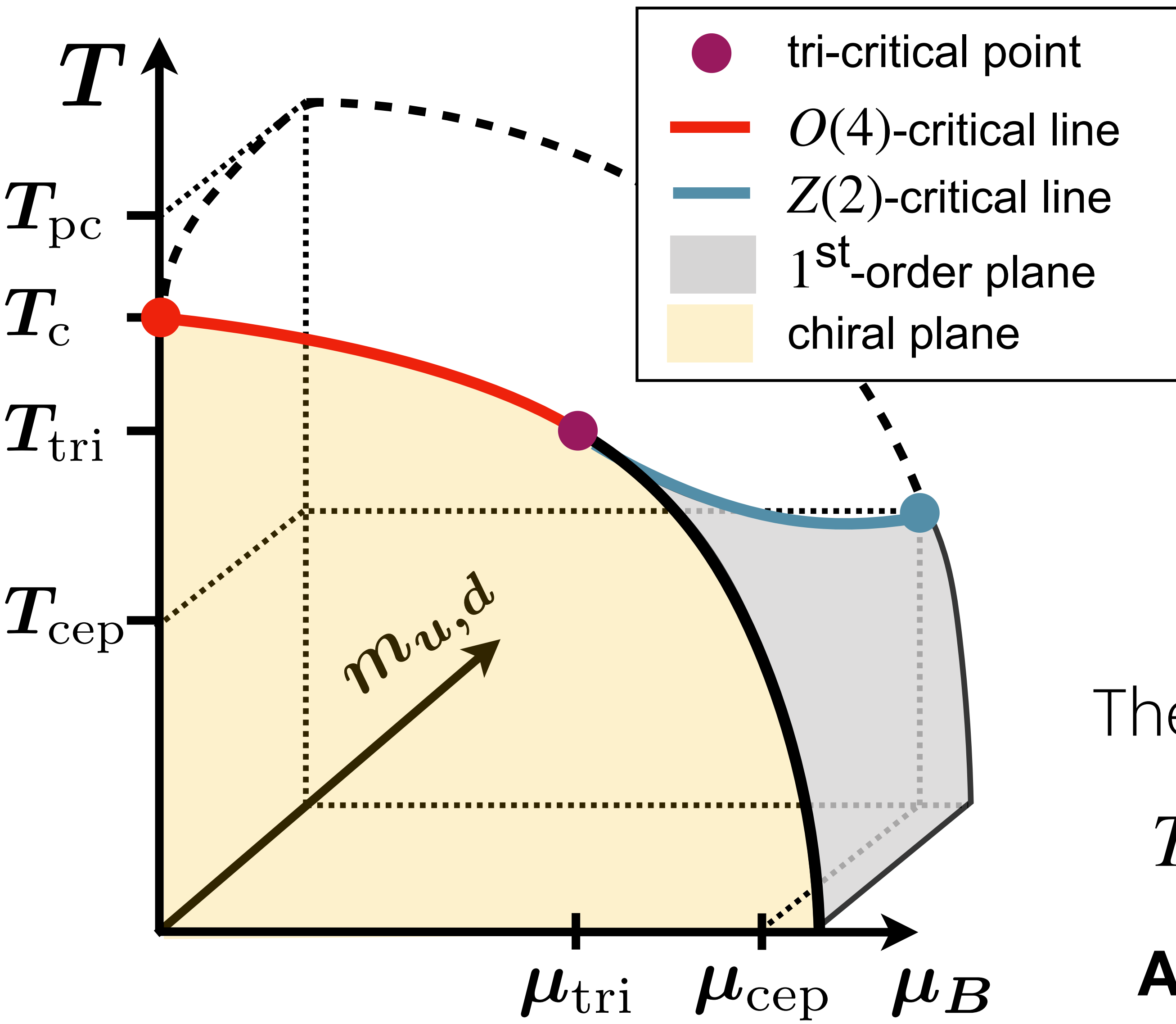

The parametrization of the pseudo-critical line of QCD :

$$T_{pc}(\mu_B) = T_{pc,0}\left[1 - \kappa_2 \hat{\mu}_B^2 + \kappa_4 \hat{\mu}_B^4\right]$$

$T_{pc,0} = (156.5 \pm 1.5)$ MeV, $\kappa_2 = 0.012(4), \kappa_4 = 0.000(4)$

$$\mu_B = \frac{T_{pc}(\mu_B)}{\sqrt{0.012}}\sqrt{1 - \frac{T_{pc}(\mu_B)}{156.5 \text{ MeV}}}$$

The upper bound of CEP is, $T_{CEP} < T_{tri} < T_c$

$T_c = 132^{+3}_{-6}$ MeV, κ_2^{χ} **= 0.015(1)**

Assuming tri-critical point exist above,

$\mu_B/T \geq 2, T_{tri} \sim 125$ MeV.

An upper bound on the CEP is, $T \sim 125$ MeV, $\mu_B \sim 510$ MeV.

[Halasz et al,arXiv:hep-ph/9804290] ; Ding et al, Phys.Rev.D 109 (2024) 114516;

Bound on the QCD critical point

CRC-TR 211

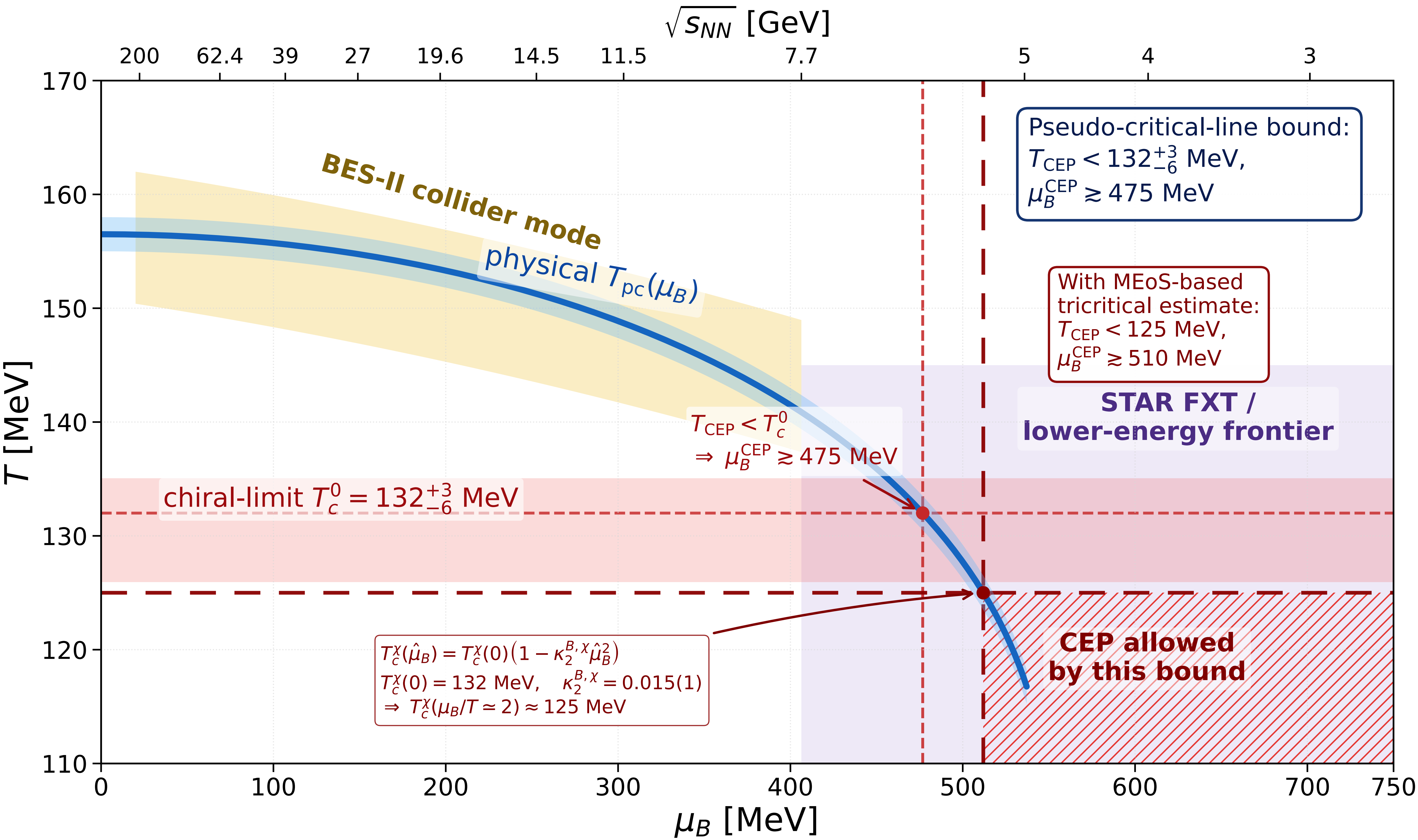

Ding et al, *Phys.Rev.D* 109 (2024) 11, 114516, A. Bazavov *et al Phys.Lett.B* 795 (2019) 15-21

Taylor expansion at finite chemical potentials

- Direct lattice QCD at real $\mu_B \neq 0$ is obstructed by the sign problem; Taylor expansion provides a controlled finite density EoS at finite chemical potentials.
- $$Z(T, V, \mu_B) = \int \mathcal{D}U\, e^{-S_g[U]} \det M(U, \mu_B),$$

  $\mu_B \in \mathbb{R}$: $\det M(U, \mu_B) \in \mathbb{C}$ $\Rightarrow$ no positive probability weight
- $$P_{2k}(T) = \frac{1}{(2k)!} \frac{\partial^{2k}}{\partial \hat{\mu}_B^{2k}} \left(\frac{p}{T^4} \right) \Bigg|_{\hat{\mu}_B = 0}, \qquad \hat{\mu}_B \equiv \frac{\mu_B}{T}$$

$$\frac{\Delta p}{T^4} = P_2(T)\hat{\mu}_B^2 + P_4(T)\hat{\mu}_B^4 + P_6(T)\hat{\mu}_B^6 + P_8(T)\hat{\mu}_B^8 + \mathcal{O}(\hat{\mu}_B^{10})$$

Coefficients are also conserved charge cumulants. Finite-density observables constructed order by order

Hadron resonance gas: low-temperature baseline for conserved-charge cumulants

- At low temperature we compare conserved-charge cumulants and Taylor coefficients with non-interacting hadron resonance gas models:

$$\frac{p^{\mathrm{HRG}}}{T^4} = \sum_{i\in\mathrm{hadrons}} \frac{p_i(T)}{T^4} \cosh\left(B_i\hat{\mu}_B + Q_i\hat{\mu}_Q + S_i\hat{\mu}_S\right).$$

- PDG-HRG: established PDG states, mainly 3-star and 4-star hadrons.
- QMHRG2020: PDG states plus additional quark-model predicted resonances, with care taken to avoid double counting.

High T perturbation theory

- At high temperature we compare the Taylor coefficients with the Stefan-Boltzmann limit and the leading $O(g^2)$ perturbative result : $\dfrac{p}{T^4} = \hat{p}_{\rm id} - g^2 \hat{p}_2,$

$$\hat{p}_{\rm id} = \frac{8\pi^2}{45}\left(1 + \frac{21 n_f}{32}\right) + \sum_{f=u,d,s}\left[\frac{1}{2}\left(\frac{\mu_f}{T}\right)^2 + \frac{1}{4\pi^2}\left(\frac{\mu_f}{T}\right)^4\right]$$

$$\hat{p}_2 = \frac{1}{6}\left(1 + \frac{5 n_f}{12}\right) + \frac{1}{2\pi^2}\sum_{f=u,d,s}\left[\frac{1}{2}\left(\frac{\mu_f}{T}\right)^2 + \frac{1}{4\pi^2}\left(\frac{\mu_f}{T}\right)^4\right]$$

$g^2(T)$ **is taken as the two-loop running coupling with** $n_f = 3$

$$\bar{\mu} = k_T \pi T, \quad 4 \le k_T \le 8, \quad \Lambda_{\overline{\rm MS}} = 339(12)\ {\rm MeV}\,.$$

CRC-TR 211

Net-baryon cumulants on the pseudo-critical line are compared with net-proton cumulants measured by STAR.

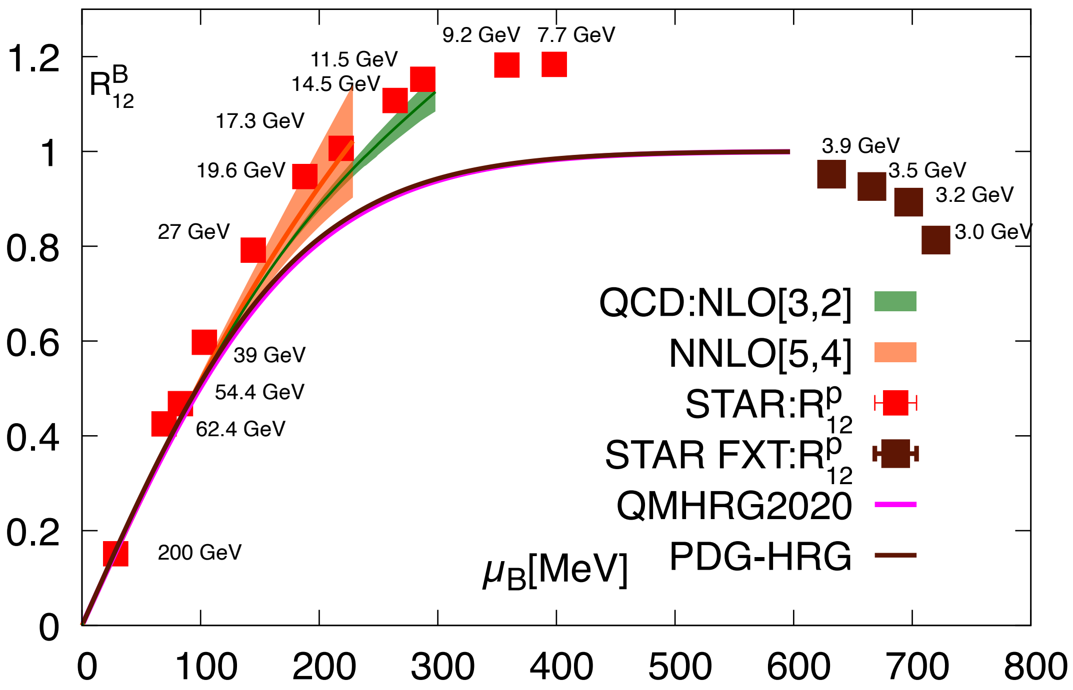

- **In good agreement with the STAR data down to $\sqrt{s_{NN}} \simeq 11.5$ GeV.**
- R^p_{12} **becomes larger than unity for $\sqrt{s_{NN}} \leq 17.3$ GeV.**
- **Consistent with QCD but not consistent with non interacting HRG.**

- $R^B_{31} = S_B\sigma^3_B$ **and** $R^B_{42} = \kappa_B\sigma^2_B$ **ratios of net baryon-number fluctuations on the pseudo-critical line of QCD.**
- **Good agreement between STAR and QCD results for $\sqrt{s_{NN}} \geq 19.6$ GeV.**

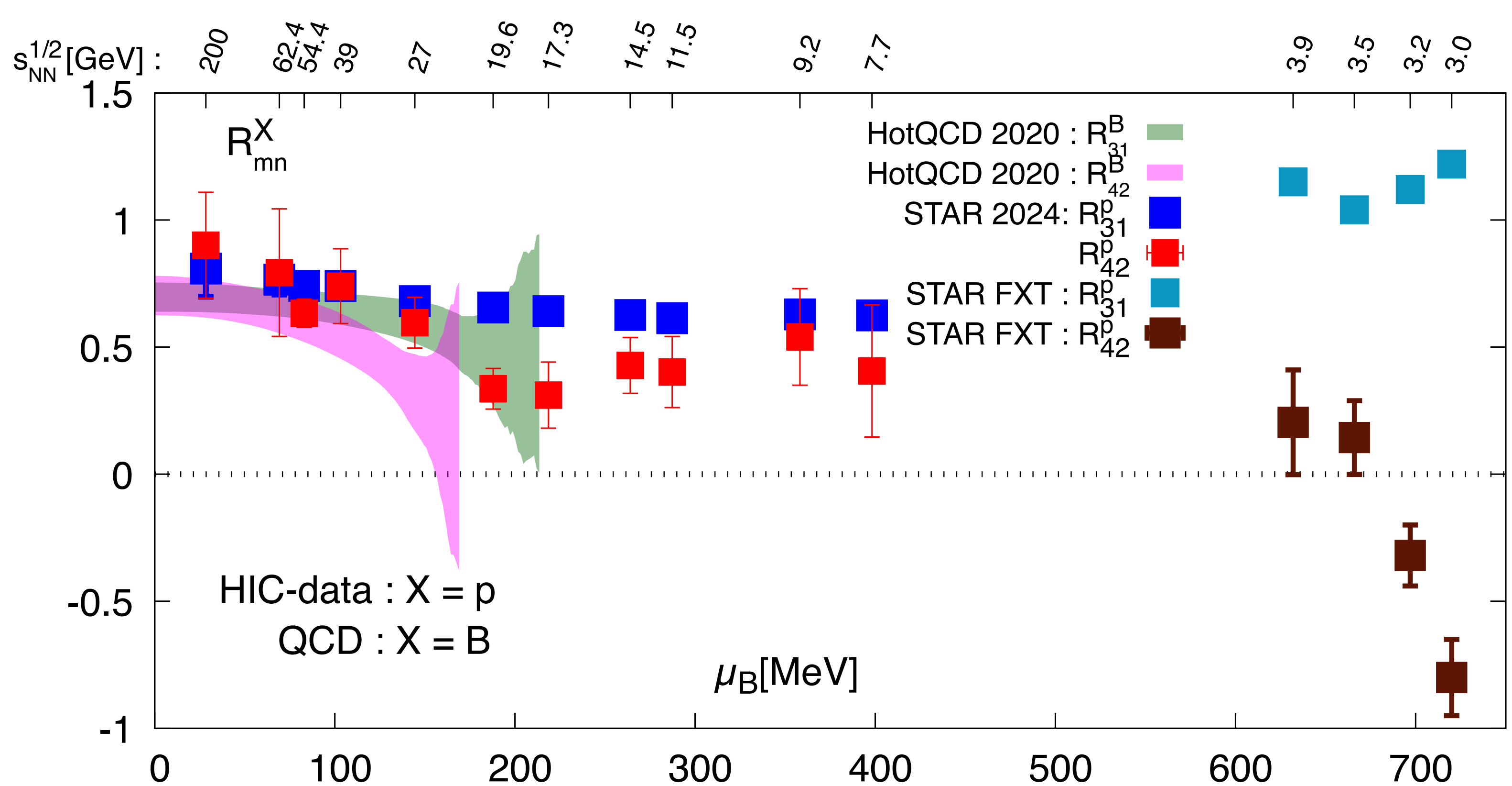

PRL135, 142305(2025),STAR FXT : Z. Sweger, QM2025

Baryon strangeness fluctuations

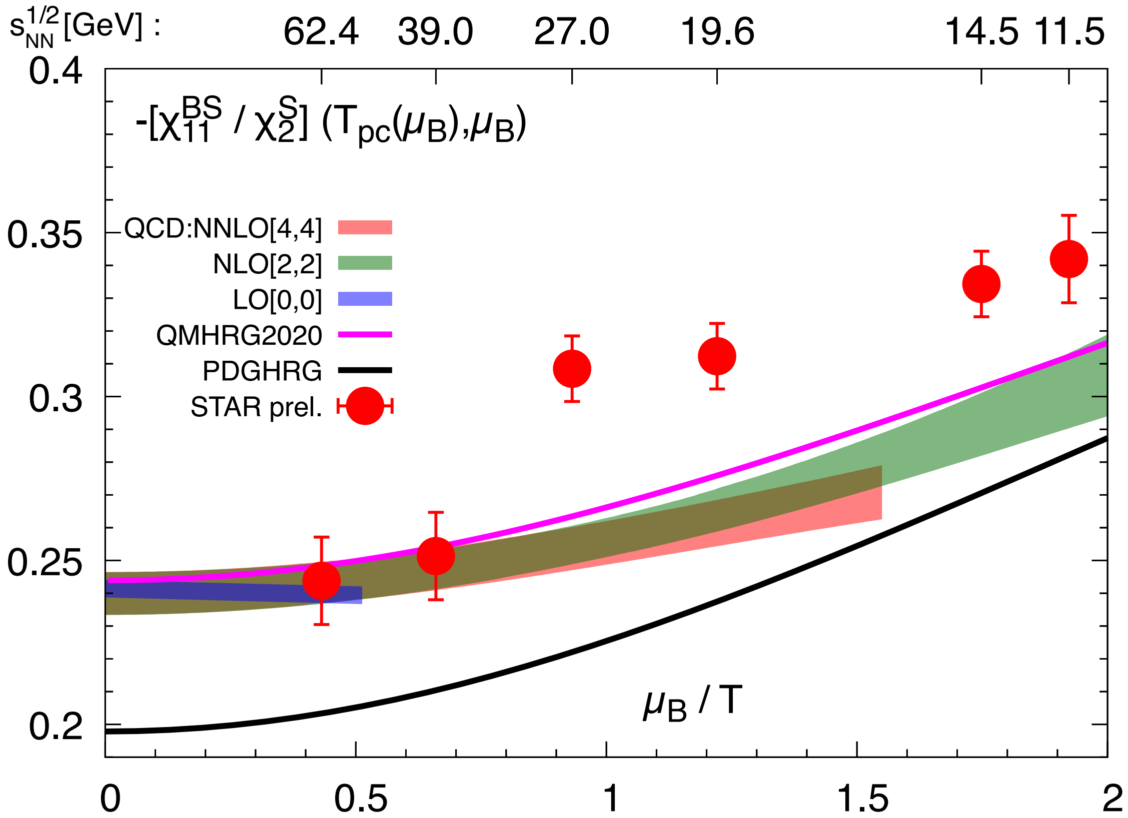

- **Baryon-strangeness fluctuations on the pseudo-critical line of QCD.**
- **Significant differences between QCD and Prelim. STAR results for $\sqrt{s_{NN}} \leq 27$ GeV.**
- **The Lattice results agree more closely with the QMHRG2020 predictions.**

- QCD sum rule :

$$2\frac{\chi_{11}^{QS}(T,\vec{\mu})}{\chi_2^S(T,\vec{\mu})} - \frac{\chi_{11}^{BS}(T,\vec{\mu})}{\chi_2^S(T,\vec{\mu})} = 1 + \frac{\Delta^{BQS}(T,\vec{\mu})}{\chi_2^S(T,\vec{\mu})}\ ;\ \vec{\mu} = (\mu_B,\mu_Q,\mu_S)$$

STAR results obtained by considering , $\Delta^{BQS}(T,\vec{\mu}) \to 0$,

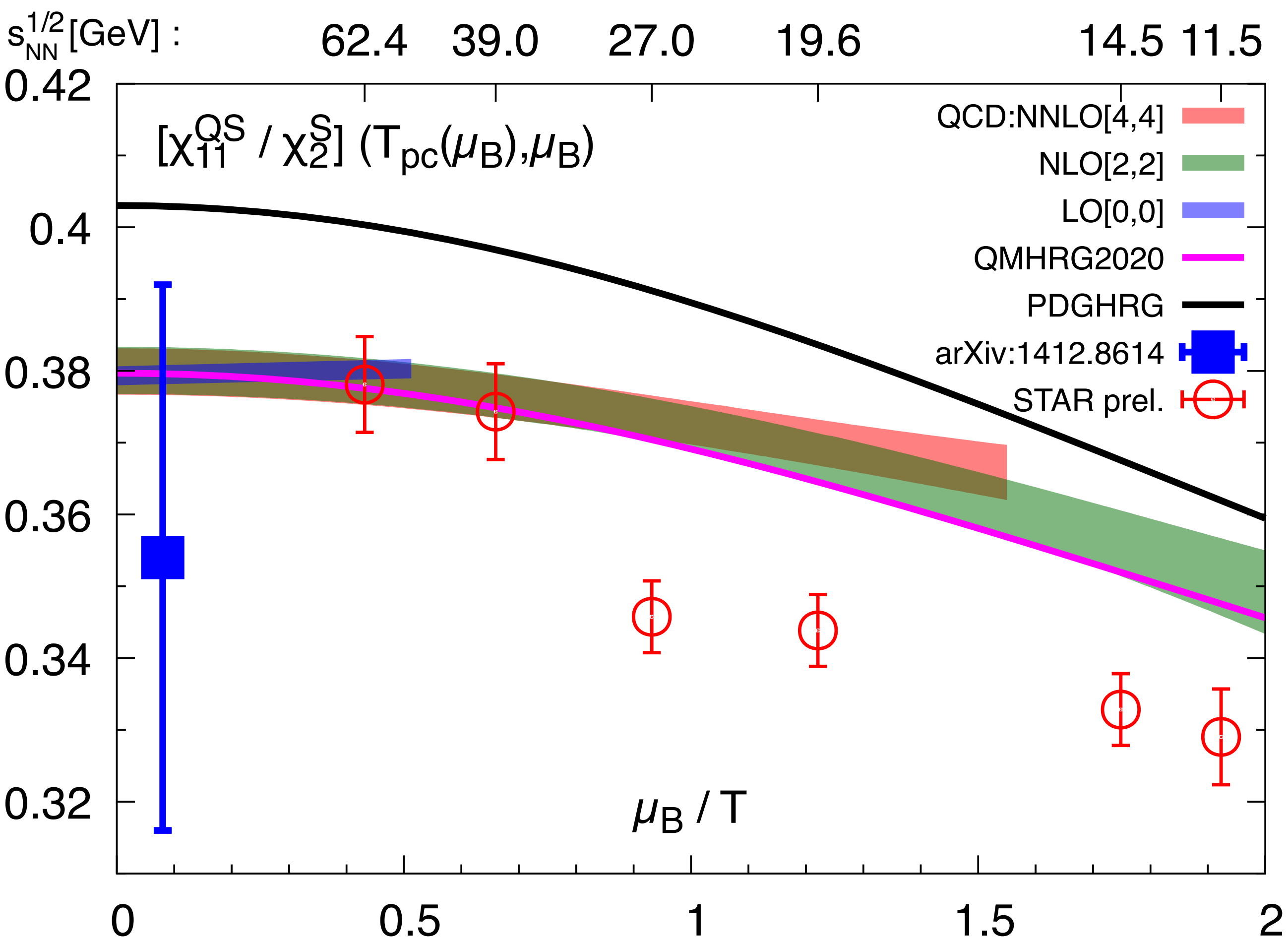

A. Bazavov et al., Phys. Rev. D101, 074502 (2020). arXiv : 2407.09335

Finite-density thermodynamics starts from $P_{2k}(T)$

- All finite-density bulk observables in this talk are generated from the temperature dependence of the Taylor coefficients of pressure, P_{2k}(T).

$$n_B,\ \epsilon,\ s, \quad \Longleftarrow \quad P_{2k}(T) \qquad n_Q/n_B = 1/2$$

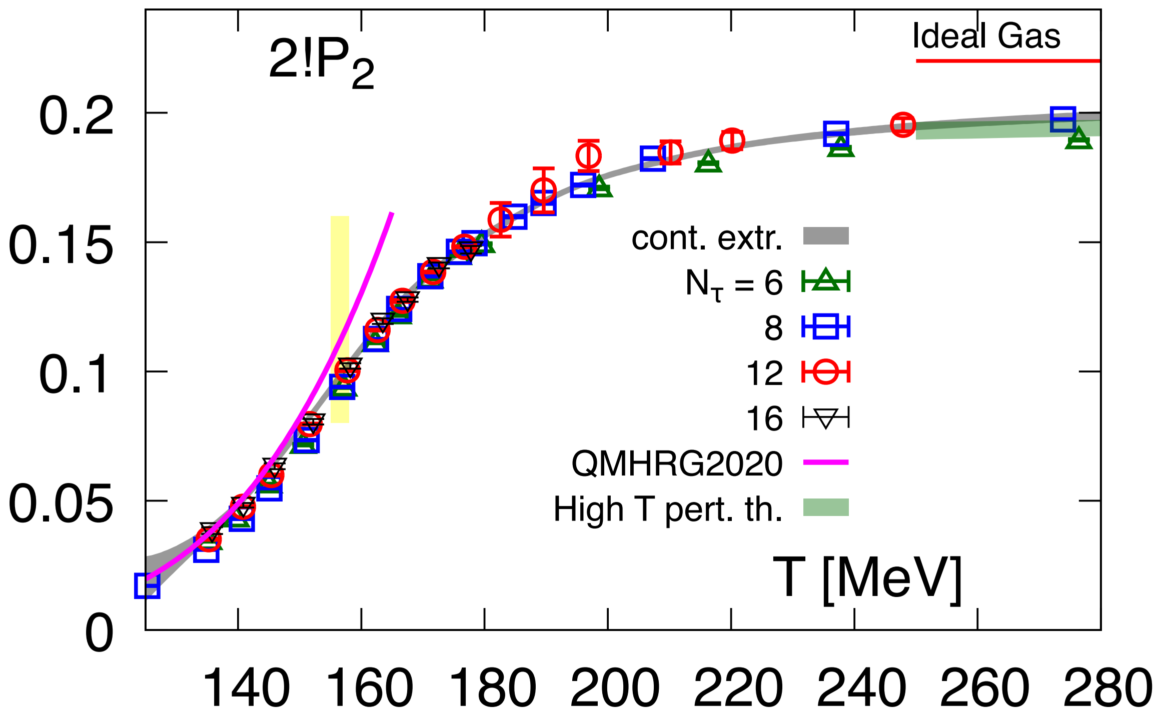

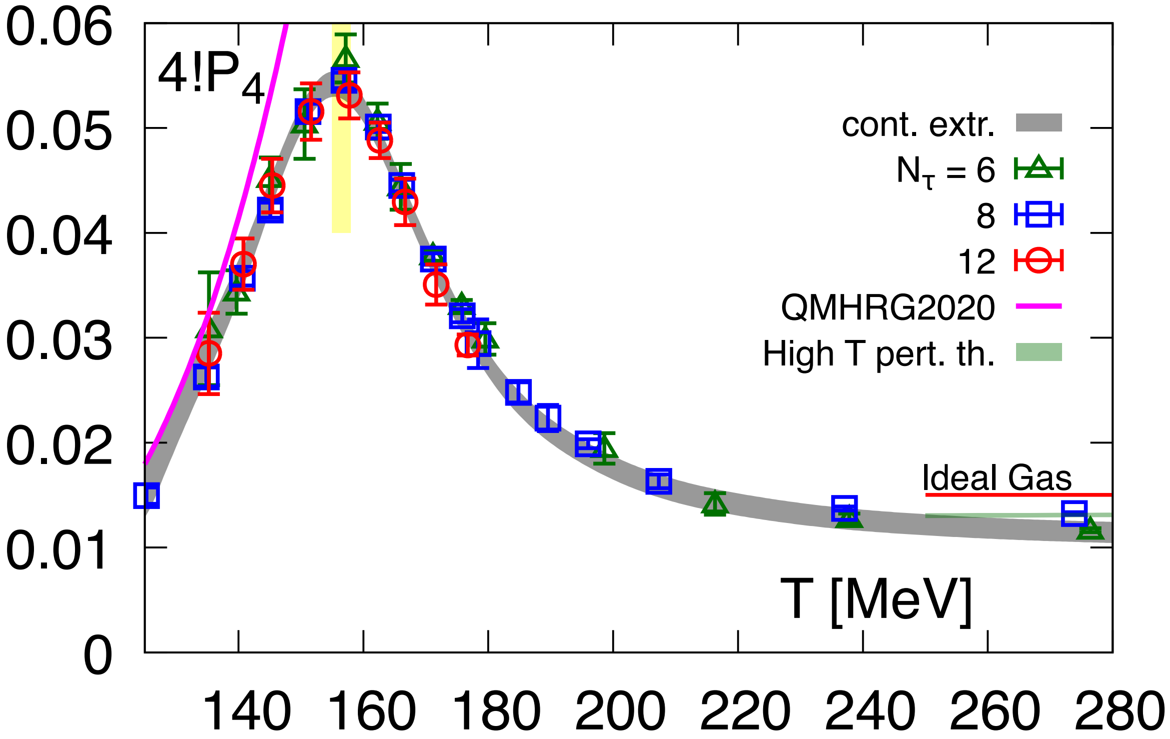

Continuum extrapolated.

HRG agreement below, $T < 145$ MeV.

Already agrees to high-T, $O(g^2)$ perturbation theory at, $T \geq 220$ MeV

D. Bollweg et al, Phys. Rev. D 108, 014510 (2023)

Finite-density thermodynamics starts from $P_{2k}(T)$

- All finite-density bulk observables in this talk are generated from the temperature dependence of the Taylor coefficients of pressure, P_{2k}(T).

$$n_B,\ \epsilon,\ s, \quad \Longleftarrow \quad P_{2k}(T) \qquad n_Q/n_B = 1/2$$

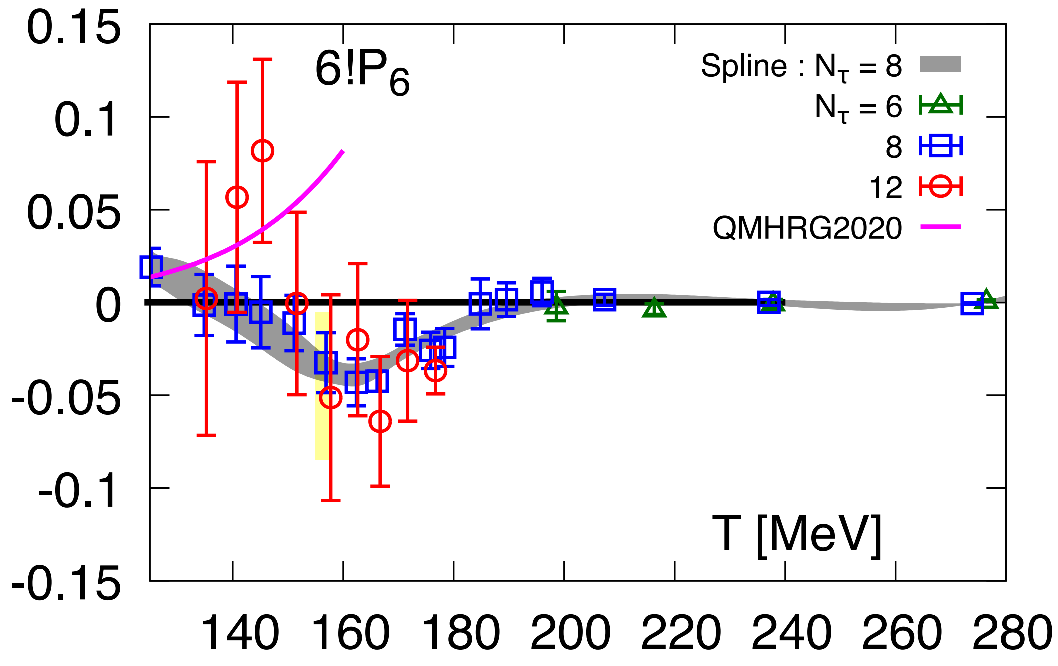

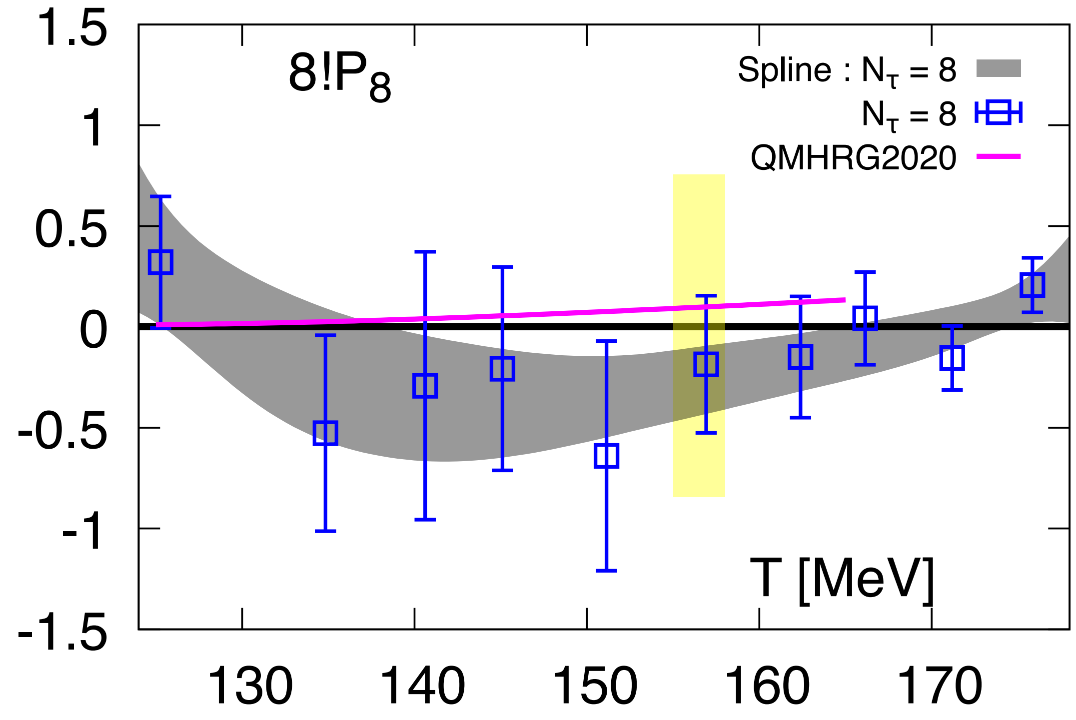

Spline interpolation only with the high statistics (1 million gauge ensembles) $N_\tau = 8$**.**

Already agrees to high-T free theory at, $T \geq 220$ MeV

Pressure at non vanishing chemical potentials

- From the Taylor coefficients we reconstruct the finite-density contribution to the pressure,
- $$\frac{\Delta p(T,\mu_B)}{T^4} \equiv \frac{p(T,\mu_B) - p(T,0)}{T^4} = \sum_{k=1}^{\infty} P_{2k}(T) \left(\frac{\mu_B}{T}\right)^{2k}$$

Setup :

$(2+1)$**-flavor QCD**, $n_S = 0,$ $n_Q/n_B = r$ $T_{pc} = 156.5(1.5)\ \text{MeV}\,.$

The pressure series generates, $n_B,\quad \epsilon,\quad s,\quad c_s^2,\quad c_T^2,\quad \kappa_T$**, by thermodynamic derivatives.**

CRC–TR 211

- $$\frac{P}{T^4} \simeq -f(T,\mu_B,m_l) \simeq f_{\mathrm{reg}}(T,\mu_B,m_l) + h^{1+1/\delta} f_f(z) \quad ,$$
  $$z = \frac{t}{h^{1/\beta\delta}}, t = \frac{1}{t_0}\left[\frac{T-T_c}{T_c} + \kappa_2^B\left(\frac{\mu_B}{T}\right)^2 + \mathcal{O}\left(\left(\frac{\mu_B}{T}\right)^4\right)\right], h = \frac{1}{h_0}\frac{m_l}{m_s}$$
- $\hat{\mu}_B^2$ enters the thermal scaling field t, baryon-number derivatives probe the same singular structure as temperature derivatives.

- $$\frac{\partial}{\partial \hat{\mu}_B^2} \sim \frac{\kappa_2^B}{t_0}\frac{\partial}{\partial t}, (P_2^s)' = T\frac{dP_2^s}{dT} \propto \kappa_2^B f_f''(z), P_4^s \propto (\kappa_2^B)^2 f_f''(z)$$
- P_2' and P_4, share the $f_f^{''}(z)$.

Pseudo-critical temperature from Taylor expansion coefficient of pressure

- $\frac{\partial}{\partial \hat{\mu}_B^2} \sim \frac{\kappa_2^B}{t_0}\frac{\partial}{\partial t}$, $\left(P_2^s\right)' = T\frac{dP_2^s}{dT} \propto \kappa_2^B f_f''(z)$, $P_4^s \propto (\kappa_2^B)^2 f_f''(z)$
- The singular parts of P_2' and P_4 are governed by the same analytic structure by $f_f''(z)$.

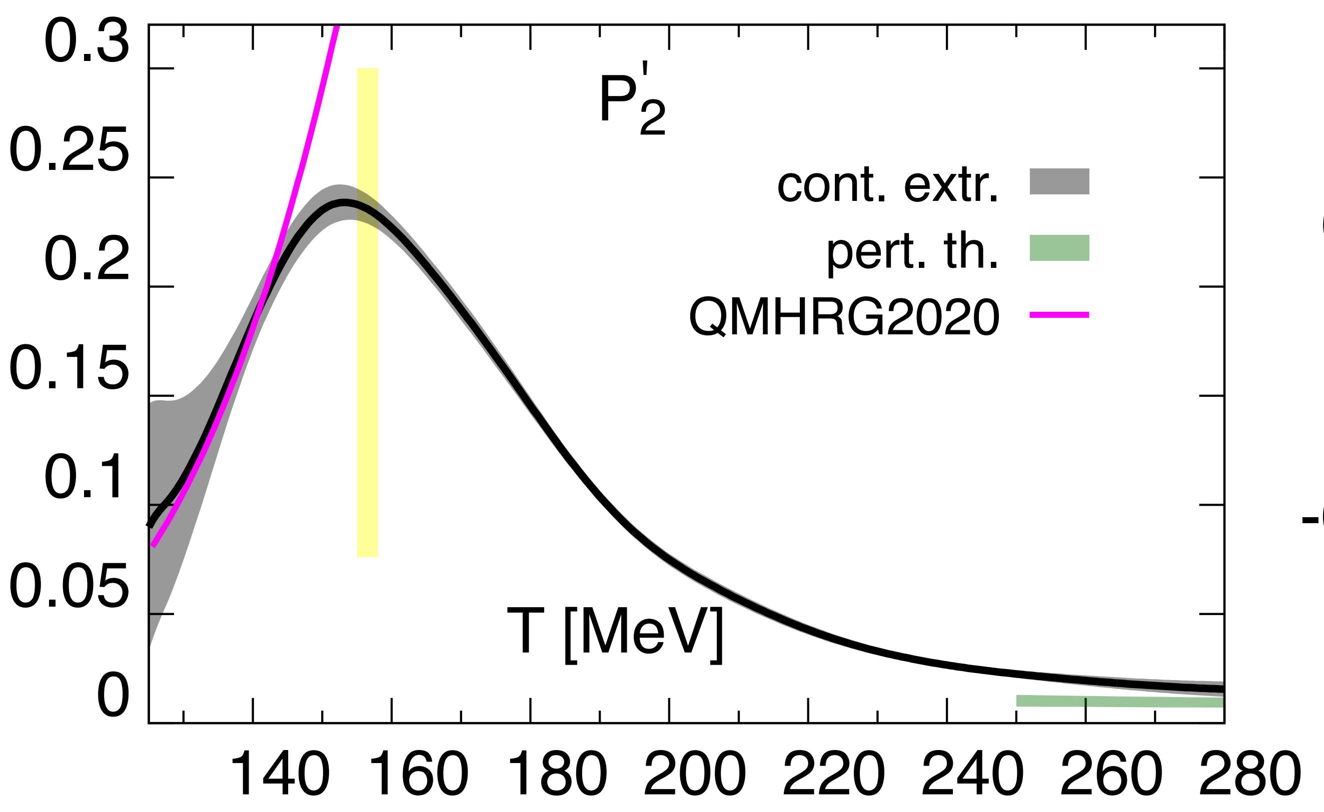

$T_{pc,0} = 153.8(7)(5)$ MeV

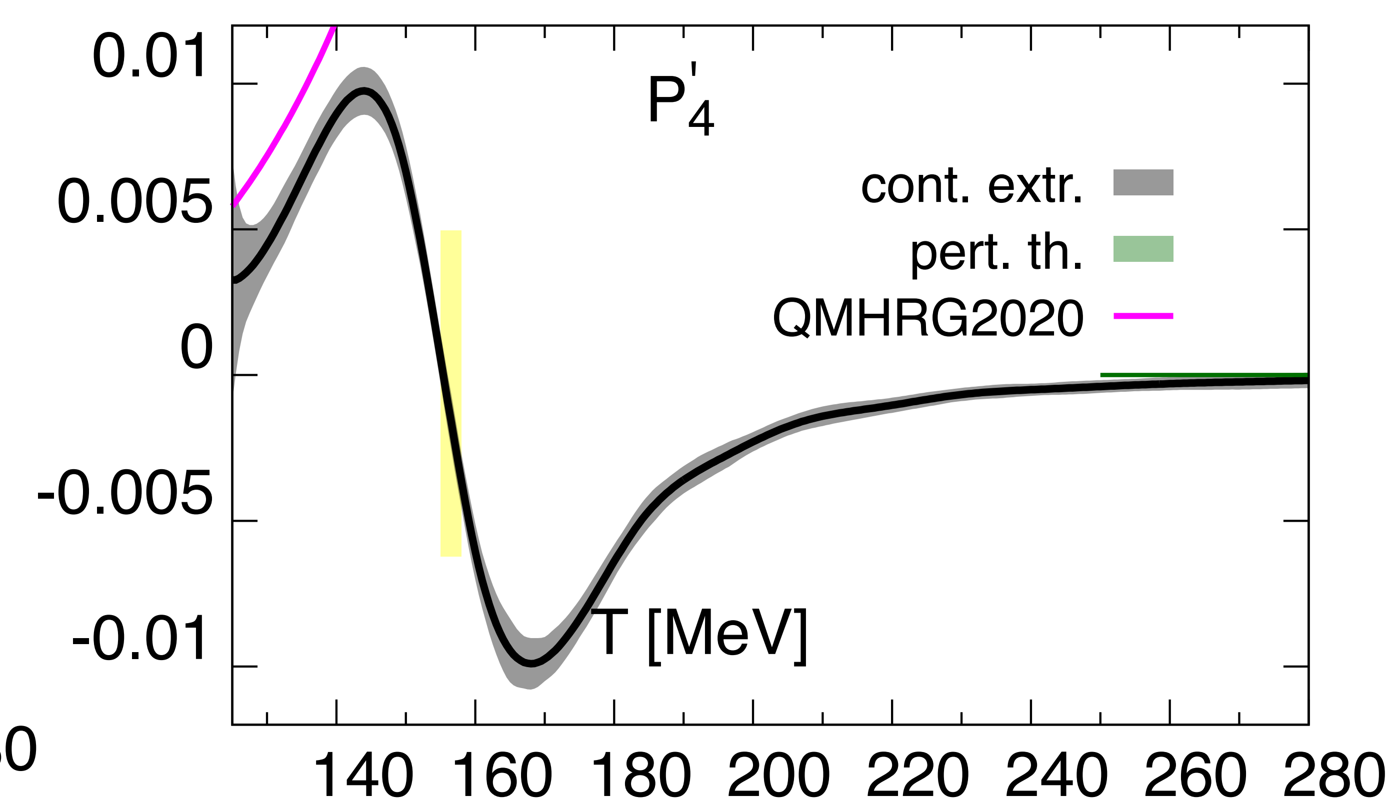

$T_{pc,0} = 155.3(2)(5)$ MeV

At physical quark masses, the transition is a crossover, so $T_{\rm pc}$ is observable dependent.

Trace anomaly at finite chemical potentials

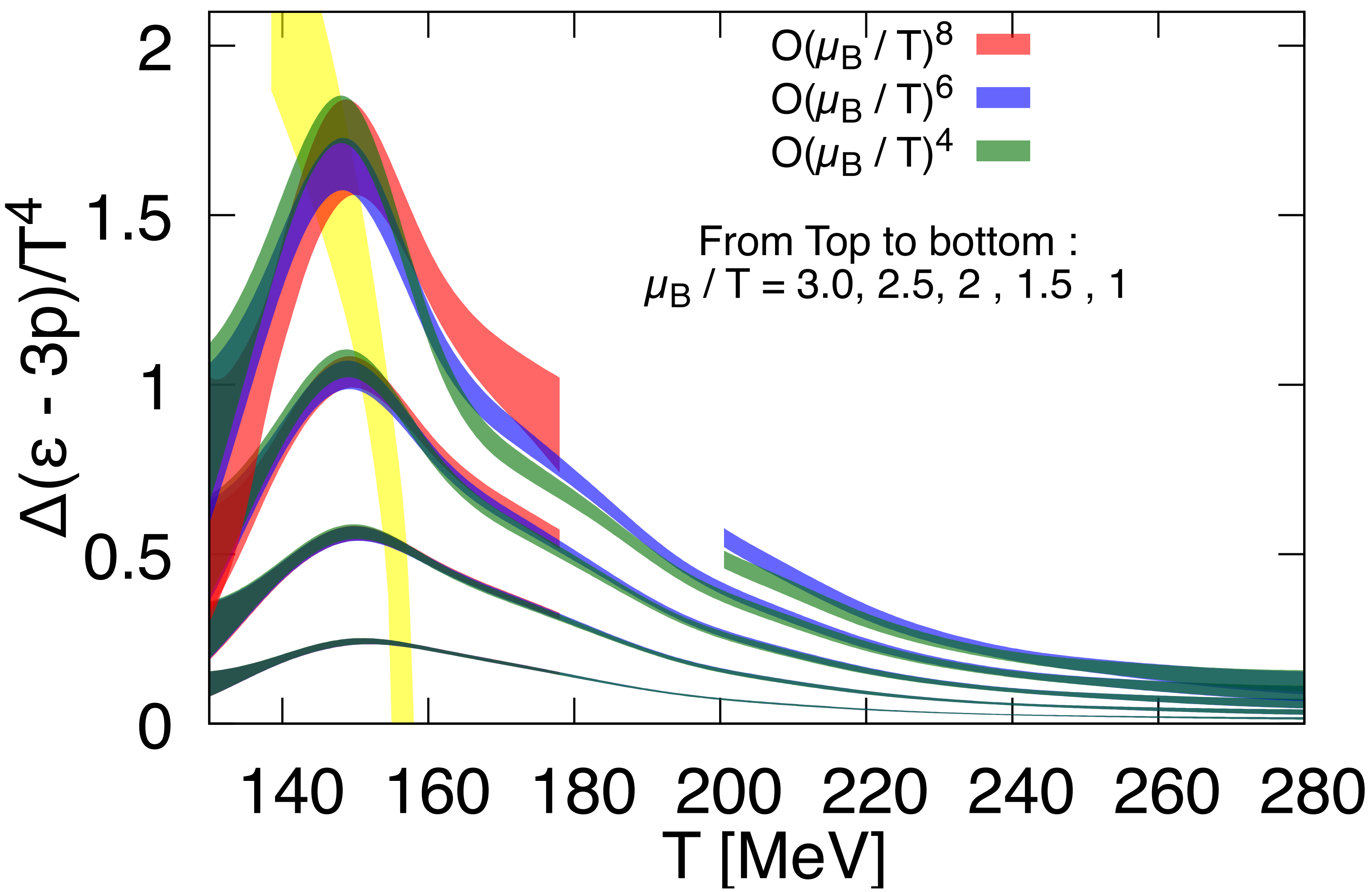

- **The finite-density trace anomaly is controlled by the thermal slopes $P'_{2k}(T) = T\, dP_{2k}/dT$.**
- **This makes $(\epsilon - 3p)/T^4$ especially sensitive to the rapid thermal variation of the EoS across the crossover.**
- **At non vanishing $\hat{\mu}_B$, the maximum violation follows the pseudo-critical line $T_{pc}(\mu_B)$.**

$$\frac{\Delta(\epsilon - 3p)}{T^4} = \sum_{k=1}^{4} P'_{2k}(T)\, \hat{\mu}_B^{2k}, \qquad P'_{2k}(T) = T\frac{dP_{2k}}{dT}.$$

Bulk thermodynamic observables

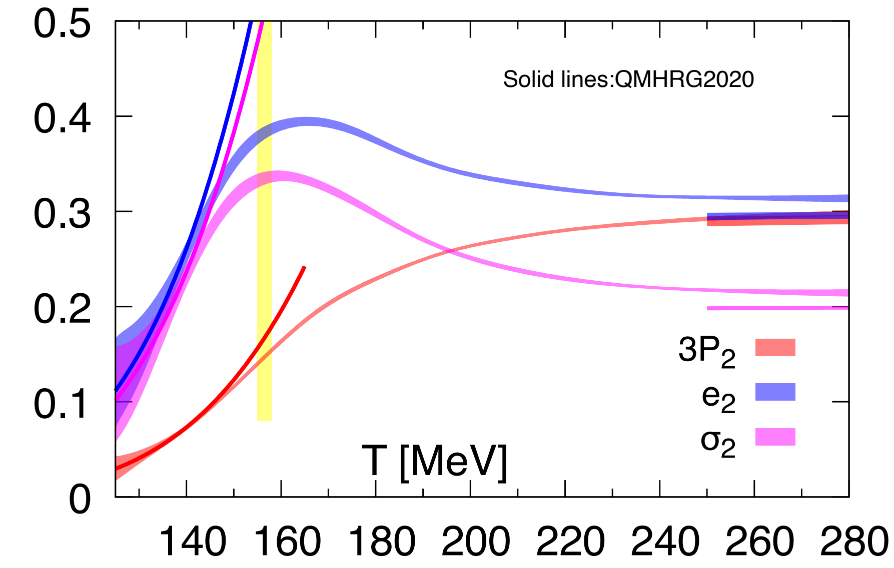

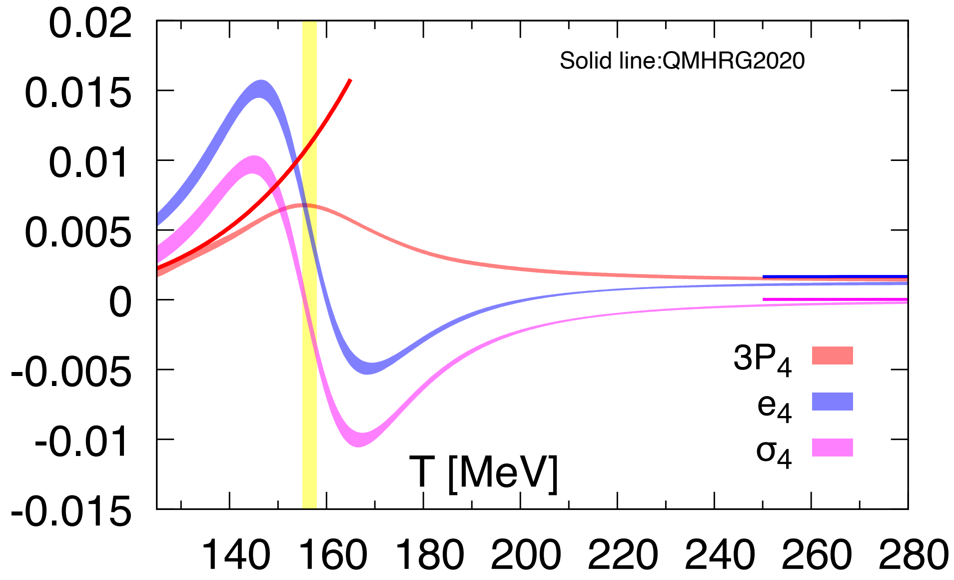

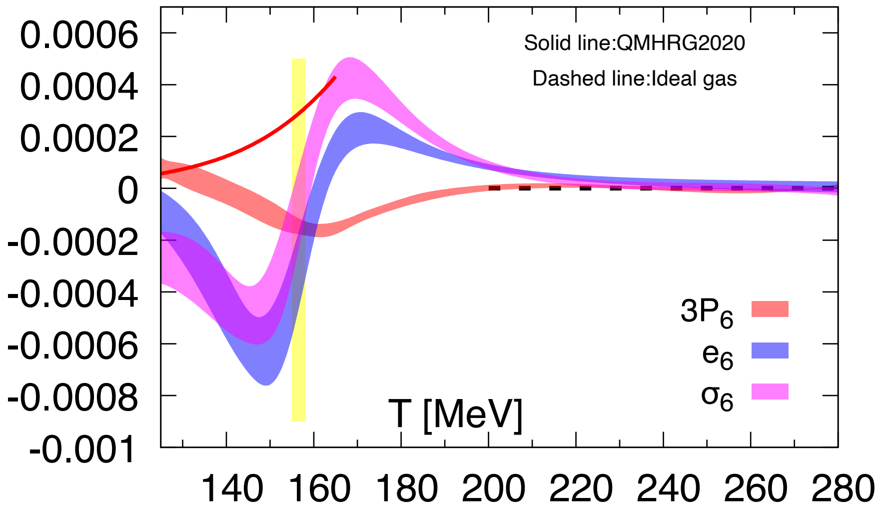

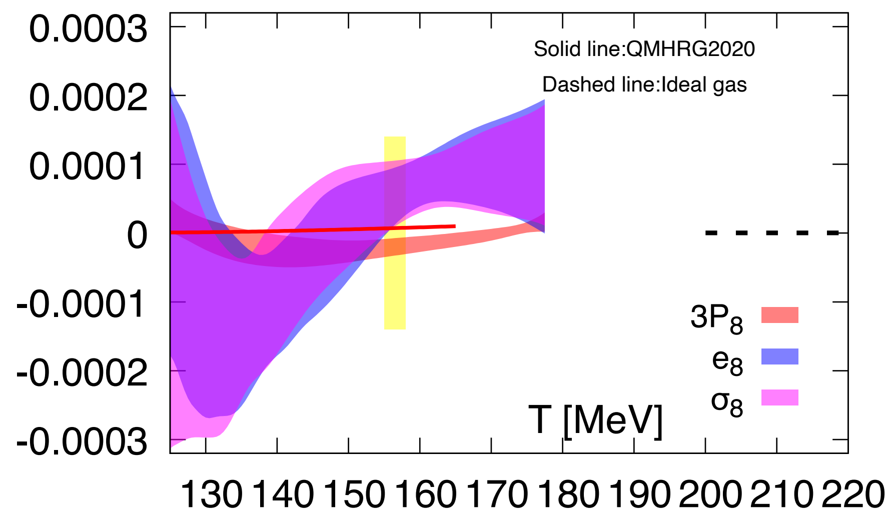

Energy and entropy coefficients are fixed by P_{2k} and its temperature derivatives,

$$\epsilon_{2k}(T) = 3P_{2k}(T) + P'_{2k}(T),\ \sigma_{2k}(T) = (4-2k)P_{2k}(T) + P'_{2k}(T) \qquad P'_{2k}(T) = T\frac{dP_{2k}}{dT}\,.$$

The second order co-efficient of energy and entropy densities are deviate from HRG earlier than pressure co-efficients.

$\hat{\mu}_B$ dependent part of the energy and entropy density

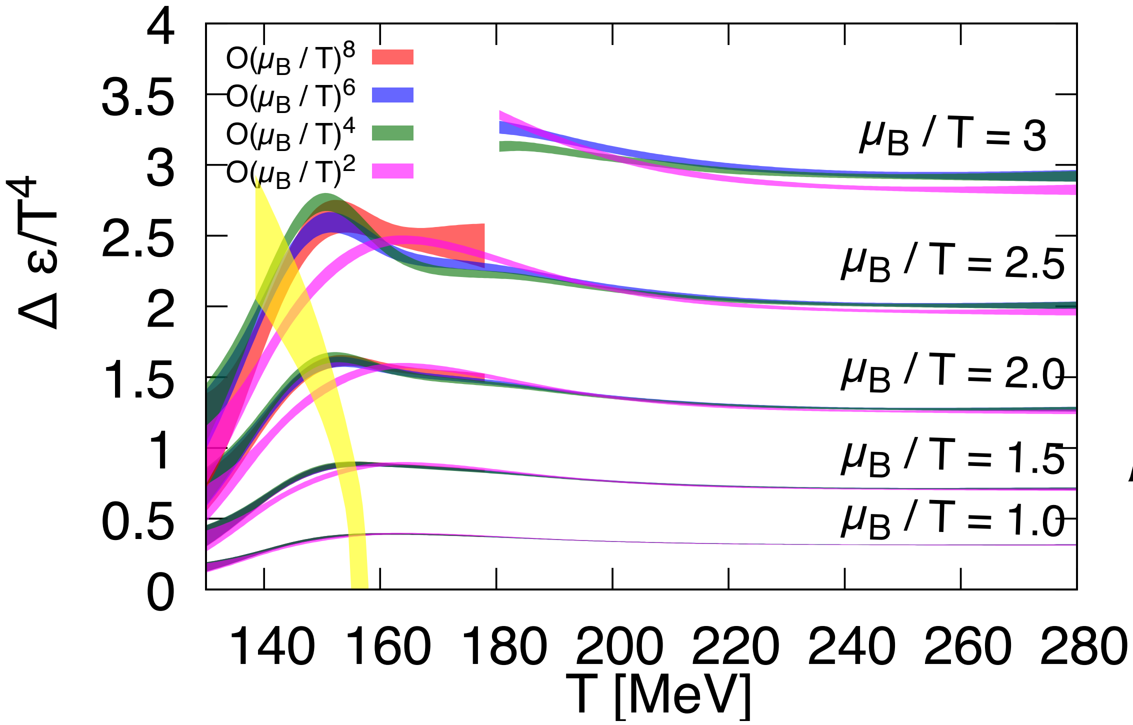

Energy and entropy densities inherit their $\hat{\mu}_B$ -dependence from $P_{2k}(T)$ and $P'_{2k}(T)$.

The fourth-order Taylor expansion works well for,

$$\hat{\mu}_B \lesssim 2.5 \quad (T \leq 150\,\mathrm{MeV}), \qquad \hat{\mu}_B \lesssim 3 \quad (T \geq 200\,\mathrm{MeV}).$$

Entropy density is the more sensitive observable at intermediate T; higher-order corrections become visible for

$$170 < T < 220\,\mathrm{MeV}, \qquad \hat{\mu}_B \gtrsim 2.5.$$

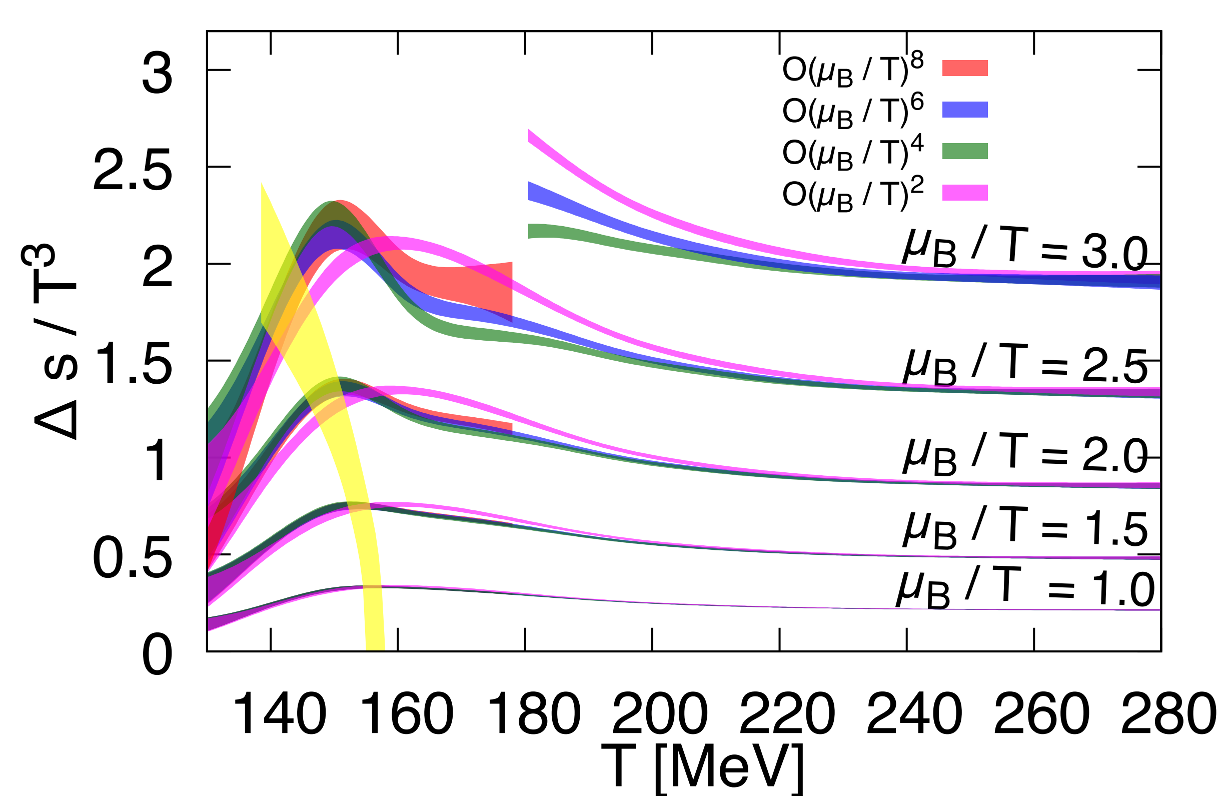

CRC-TR 211

- For any thermodynamic quantity, f, a line of constant f is written as, $T_f(\hat{\mu}_B) = T_f(0)\left[1 - \kappa_2^f\,\hat{\mu}_B^2 + \mathcal{O}(\hat{\mu}_B^4)\right]$

$$\kappa_2^\epsilon = 0.0104(12), \qquad \kappa_2^s = 0.0091(11), \qquad \kappa_2 = 0.012(4)$$

k_2^ϵ **: how fast T must decrease with** μ_B **to keep the energy density fixed.**

k_2^s **: how fast T must decrease with** μ_B **to keep the entropy density fixed.**

$$\frac{\kappa_2^s}{\kappa_2^\epsilon} = \frac{\sigma_2}{\epsilon_2} = 1 - \frac{P_2}{\epsilon_2} = 0.872(3)(5)$$

$\kappa_2^\epsilon > \kappa_2^s \quad \Rightarrow$ **iso-ϵ line bends slightly more than iso-s line**

$$\epsilon\left(T_{pc}\right) \simeq 370(40)(30)\ \mathrm{MeV/fm^3} \quad \longrightarrow \quad 330(28)(53)\ \mathrm{MeV/fm^3}$$

$$\hat{\mu}_B = 0 \quad \longrightarrow \quad \hat{\mu}_B = 2.5$$

The lattice crossover line is not just a line in the $T - \mu_B$ plane, thermodynamically, it lies close to lines of constant energy and entropy density.

How dense is the QCD matter accessible from Taylor expansions??

$$\hat{n}_B = N_1\hat{\mu}_B + N_3\hat{\mu}_B^3$$

The $O((\mu_B/T)^3)$ truncation provides a reliable description of $\hat{n}_B$ up to,

$\mu_B/T = 2.5\ ,T \leq 150\ \mathrm{MeV};$

$\mu_B/T = 2,\ 150\ \mathrm{MeV} < \mathrm{T} < 200\ \mathrm{MeV};$

$\mu_B/T = 3,\ T \geq 200\ \mathrm{MeV}$

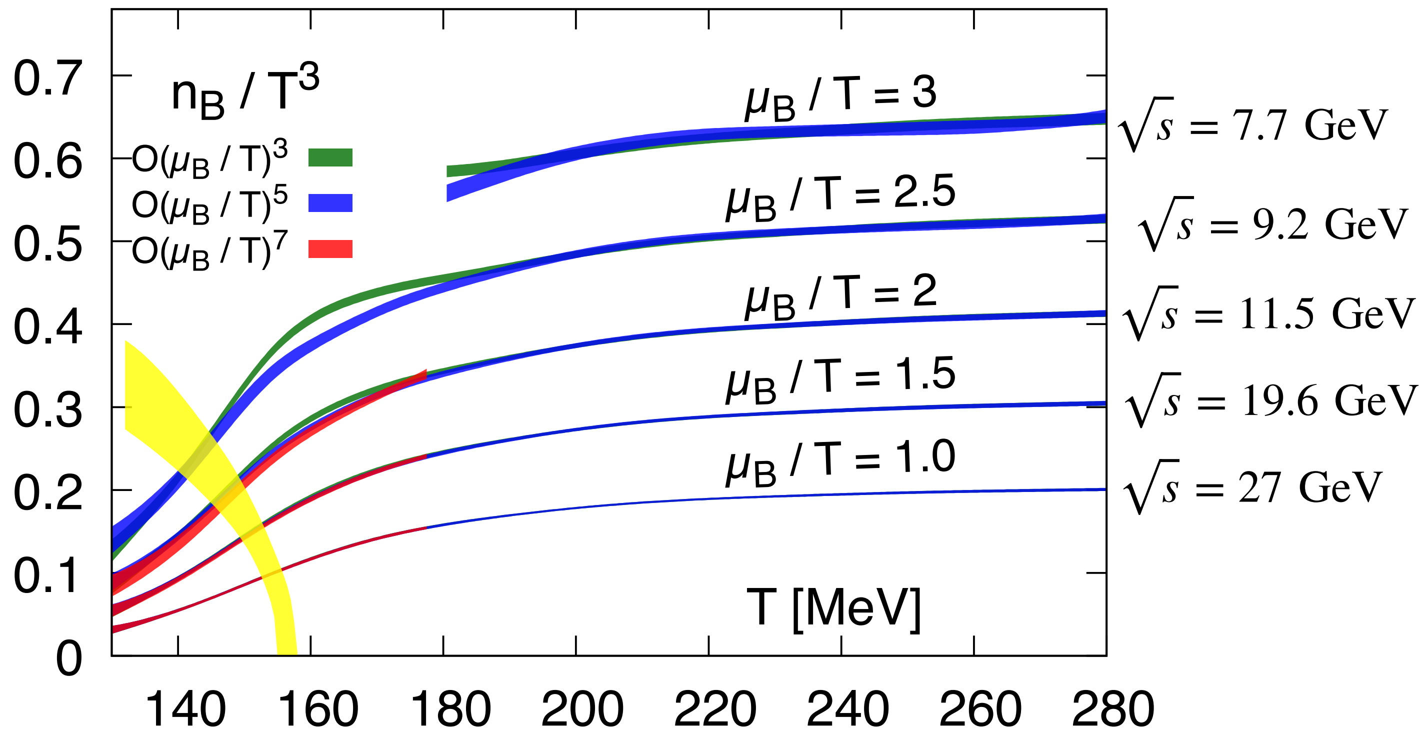

D. Bollweg et al, Phys. Rev. D 108, 014510 (2023)

How does finite-density QCD matter respond to compression and heating?

CRC-TR 211

$$\kappa_T = -\frac{1}{V}\left(\frac{\partial V}{\partial P}\right)_{T,N}$$

Response of the volume to compression at fixed T.

$$\alpha_T = \frac{1}{V}\left(\frac{\partial V}{\partial T}\right)_{p,N}$$

Response of the volume to heating at fixed pressure.

$$c_V = \frac{T}{V}\left(\frac{\partial S}{\partial T}\right)_{V,N}$$

Heat required to raise T at fixed volume.

$$c_P = \frac{T}{V}\left(\frac{\partial S}{\partial T}\right)_{P,N}$$

Heat required to raise T at fixed pressure.

In textbook thermodynamics these are usually defined at fixed total particle number, N.
In QCD the natural fixed quantities are net conserved charges or net densities (n_B, n_Q, n_S).

c_s^2, c_T^2 :adiabatic and isothermal response to compression

How does finite-density QCD matter respond to compression and heating?

- n_B/n_0 is used here as the dimensionless net-baryon density, normalized by the nuclear saturation density, $n_0 \simeq 0.16 \ \mathrm{fm}^{-3}$.
- For estimating the total thermal abundance of baryon-number carrying states, an HRG-motivated measure is instead $\dfrac{T^3\chi_2^B}{n_0}$. [Work ongoing]
- Analogously, $T^3\chi_2^Q/n_0$, provides a proxy for the total number of charged hadrons. [Work ongoing]

In this talk I will present most of the material parameters with respect to n_B/n_0.

Adiabatic sound speed in dense QCD matter

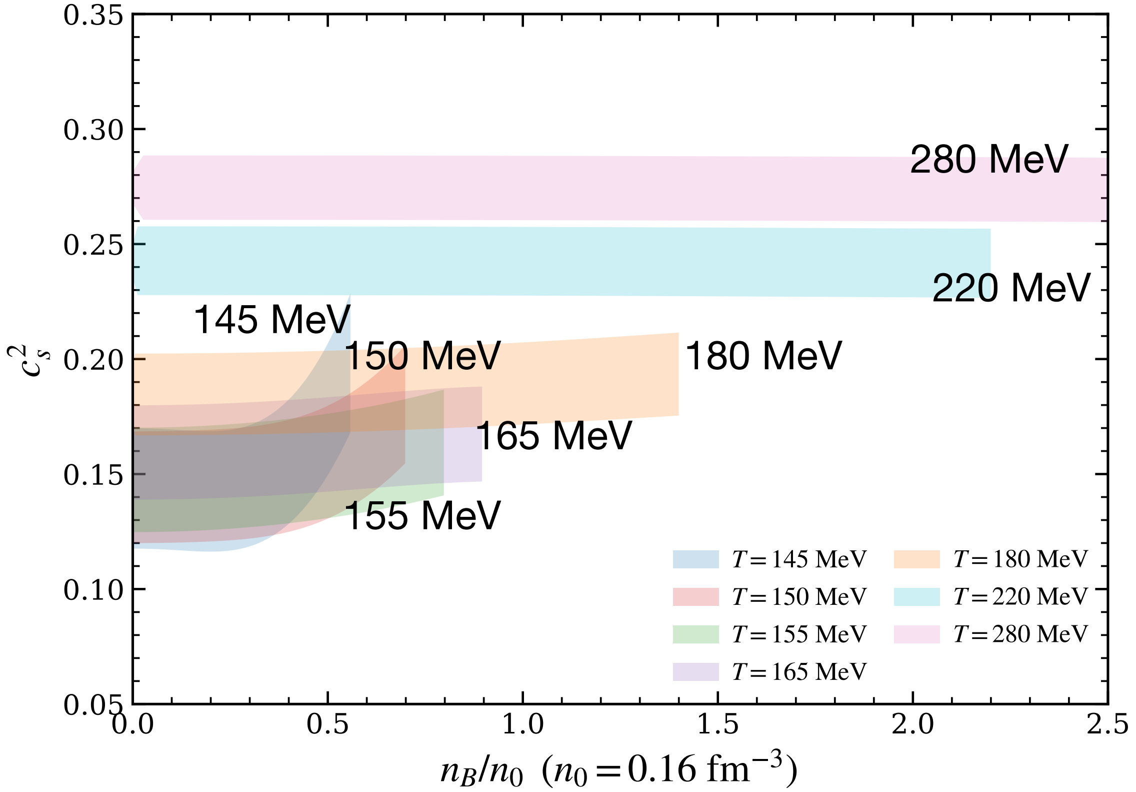

$$c_s^2 = \left(\frac{\partial P}{\partial \epsilon}\right)_{s/n_B}$$

Low T matter stiffens with increasing density, whereas high T matter is already stiff and changes only weakly with density.

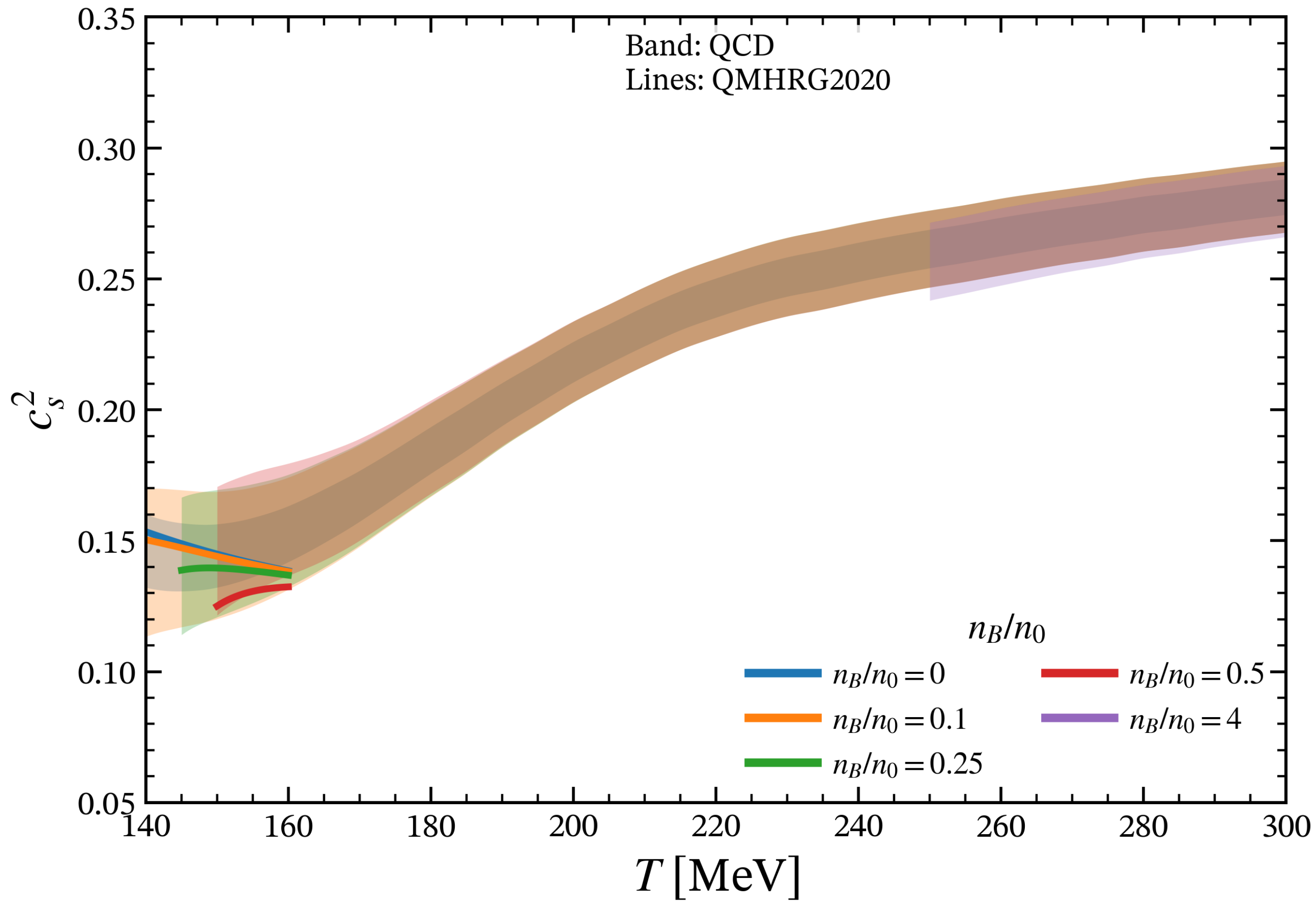

Finite-density effects are most pronounced below the QCD crossover temperature,
$T_{pc} = 156.5$ MeV.

Isothermal sound speed: compression at fixed temperature

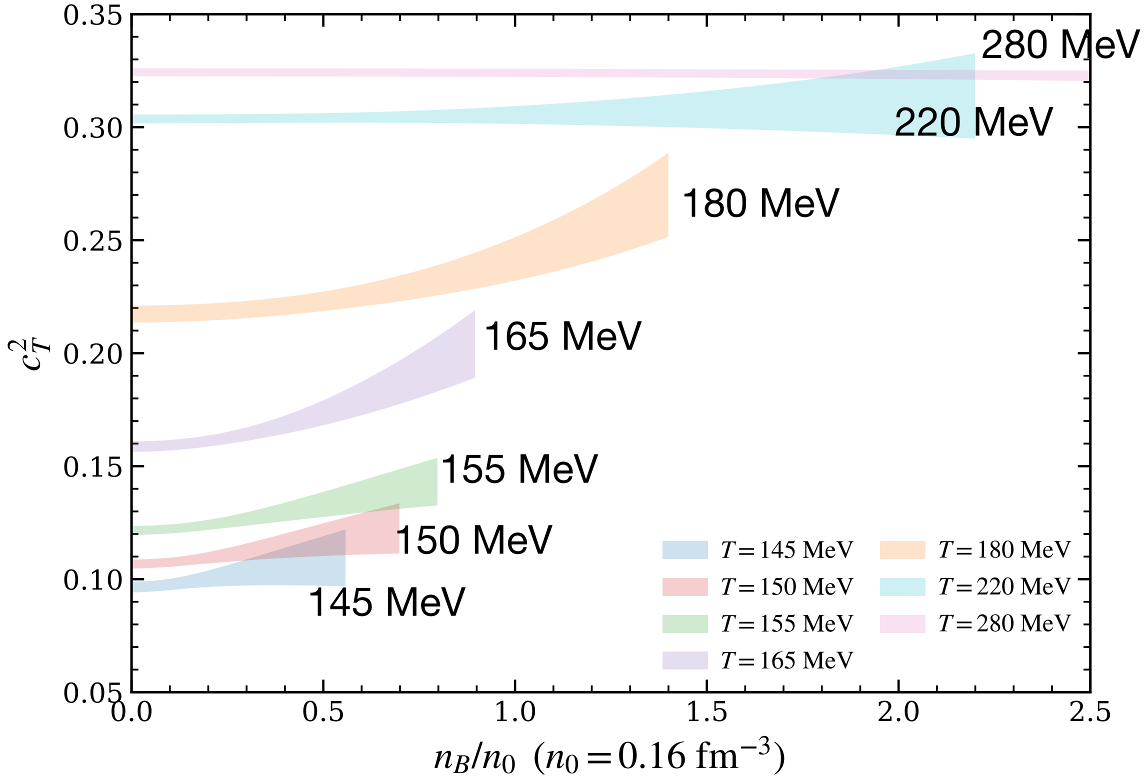

$$c_{T,F}^2 = \frac{\hat{n}_B}{3\hat{n}_B + TD_T\hat{n}_B}$$

Similar trend: Strong density dependence at low T. Weak density dependence at high T.

At, fixed, n_B/n_0 the separation between curves is largest at low T.

At higher T, the curves flatten and move closer together.

Finite-density effects are therefore most visible in the hadronic and crossover regime.

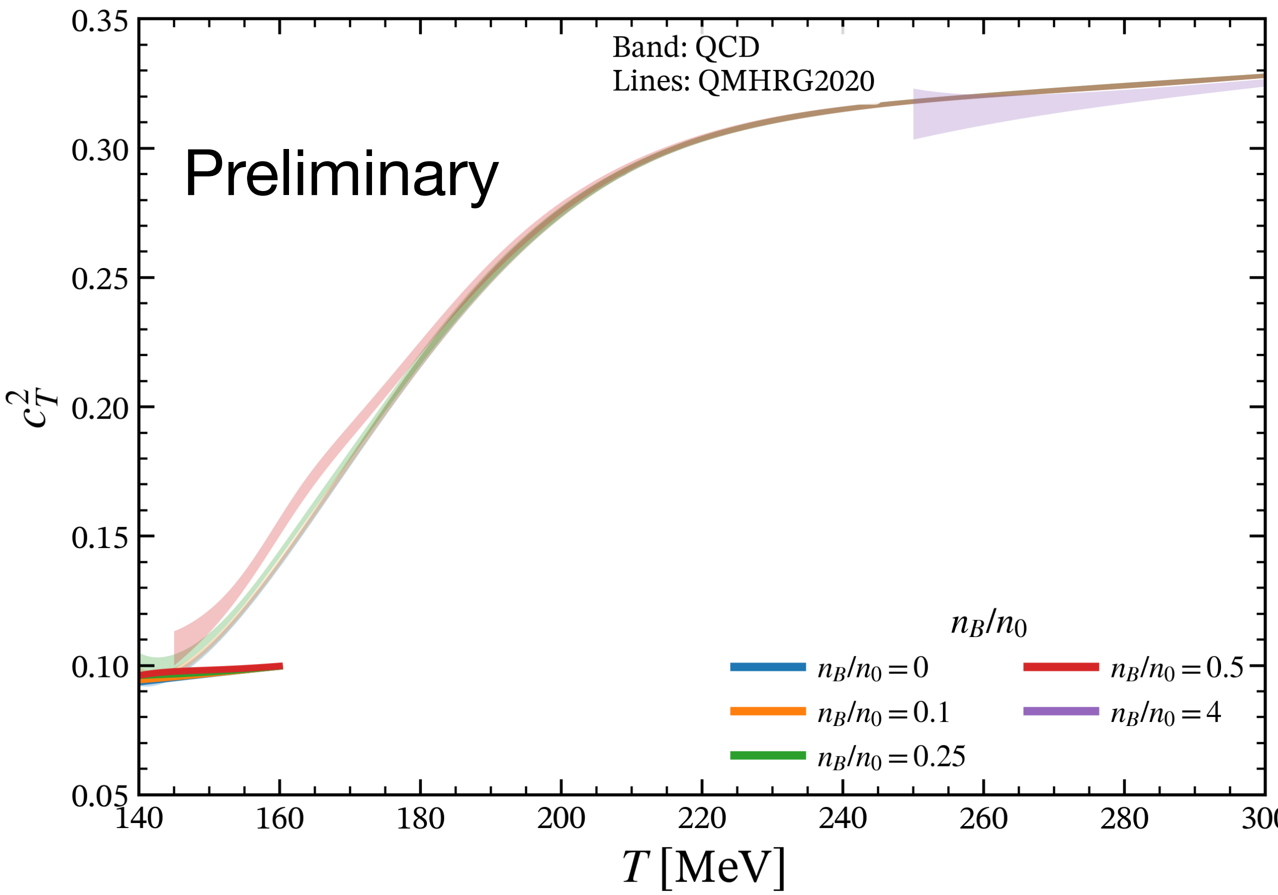

Specific heat at fixed volume(c_V/T^3)

CRC-TR 211

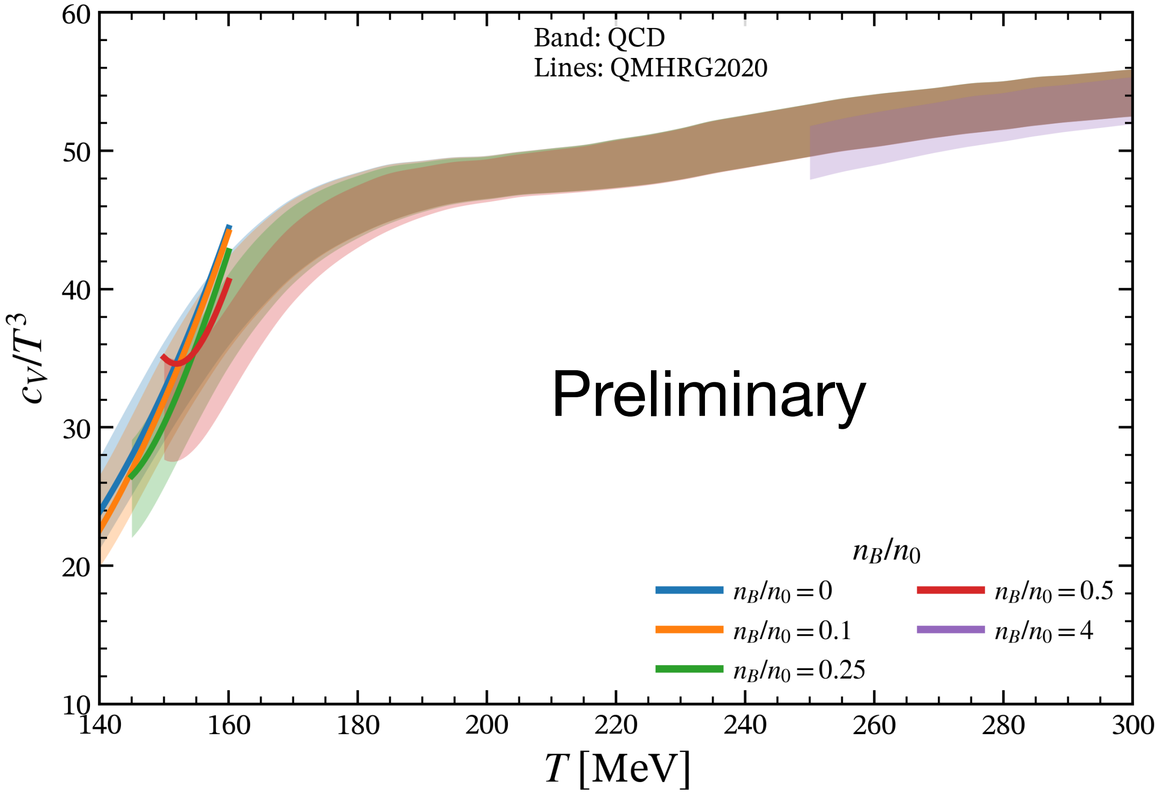

$$c_v/T^3\Big|^{singular}_{\hat{\mu}_B=0} \sim A_{+/-}\left|\frac{T-T_c}{T_c}\right|^{-\alpha}$$

For the **O(4)** universality class, $\alpha=-0.21$; Therefore in the **chiral limit** c_v/T^3 doesn't diverge but develops a cusp.

At **physical quark masses**, this singular structure is smoothed by the regular part.

In our current finite-density results, we do not observe an obvious remnant critical signature in c_v/T^3.

Moreover at finite density, we also didn't see any hint of an QCD critical point.

Isothermal compressibility in (2+1)-flavor lattice QCD

CRC-TR 211

- The Isothermal compressibility for any fixed net conserved charge density is, $\kappa_T = -\frac{1}{V}\left(\frac{\partial V}{\partial P}\right)_{T,N} = \frac{1}{T^4 \hat{n}^2}\frac{\partial^2 \hat{P}}{\partial \hat{\mu}^2} \longrightarrow$ diverges at $\mu_B \to 0$.
- We propose to fix a fluctuation like observables, (χ_2^X or $\sigma_{\mathrm{X}}^2 = \mathrm{VT}^3\chi_2^{\mathrm{X}}, X = B, Q, S$).
- At low T, $\sigma_Q^2 = N_Q + N_{\bar{Q}}$, provides a good proxy for total charge particle numbers in HRG and since the dominant contribution comes from pions.
- In this talk we fix χ_2^Q , this leads to, $\kappa_{T,\chi_2^Q} T^4 \equiv \frac{1}{\chi_2^Q}\frac{\chi_{12}^{BQ} - \frac{\chi_{11}^{BS}}{\chi_2^S}\chi_{21}^{QS}}{\hat{n}_B}$
- LO behaviour : $\chi_{12}^{BQ} \sim \hat{\mu}_B$, $\chi_{21}^{QS} \sim \hat{\mu}_B$, $\hat{n}_B \sim \hat{\mu}_B$

Isothermal compressibility at vanishing chemical potentials

- The dominant contribution at $\hat{\mu}_B = 0$ to $\kappa_T T^4$ is comes from, $\kappa_T^0(1 + \delta\kappa_T)T^4$.

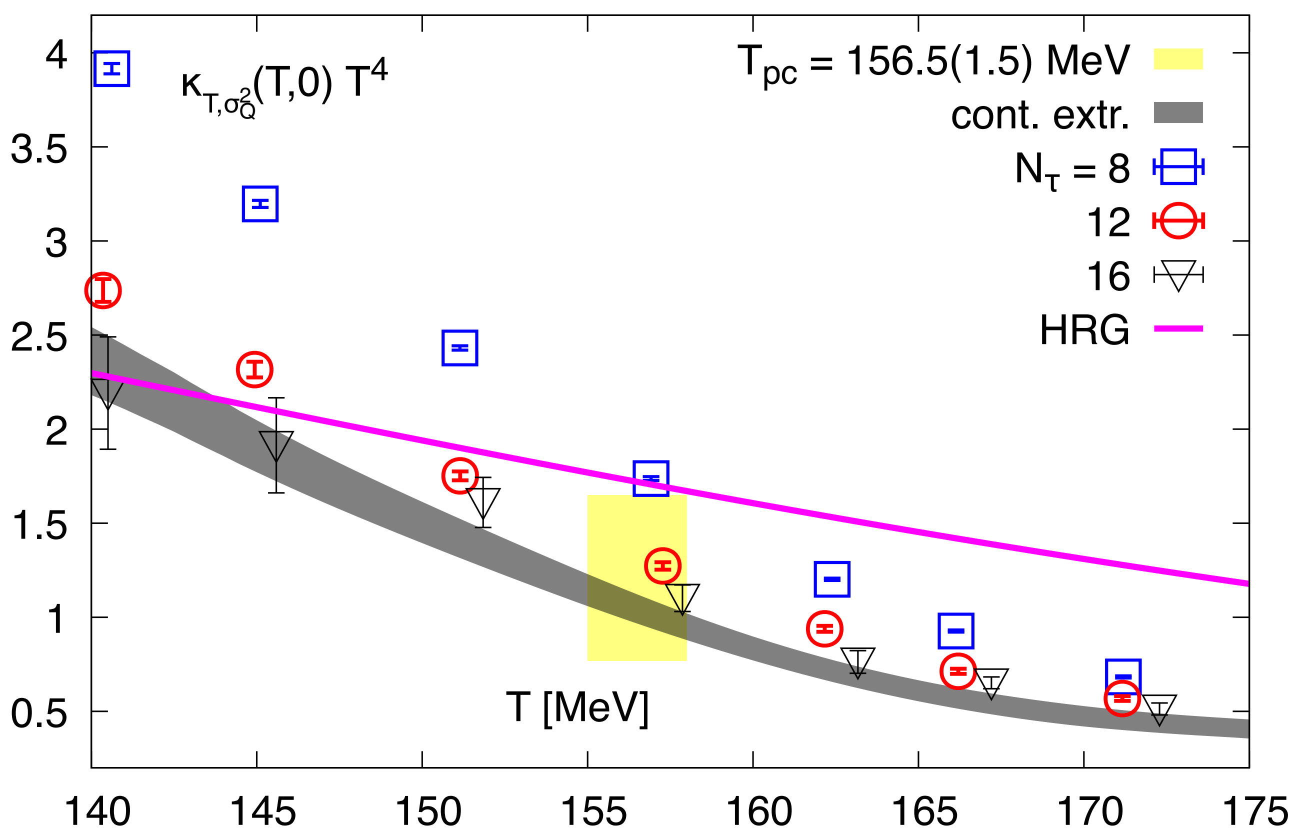

$$\kappa_T^0 = \frac{\chi_{22}^{BQ}}{\chi_2^B \chi_2^Q} \frac{1 - \frac{\chi_{121}^{BQS}\chi_{11}^{BS}}{\chi_{22}^{BQ}\chi_2^S}}{1 - \frac{(\chi_{11}^{BS})^2}{\chi_2^B \chi_2^S}}$$

Numerator : Charged baryons

Denominator : pions

Reasons for deviations from HRG :

1. Numerator : Fourth order and $\Delta^{++}, N*$ contributions.
2. Denominator : χ_2^Q deviates from HRG at the T_{pc} .

κ_T : Heavy ion data vs Lattice QCD data

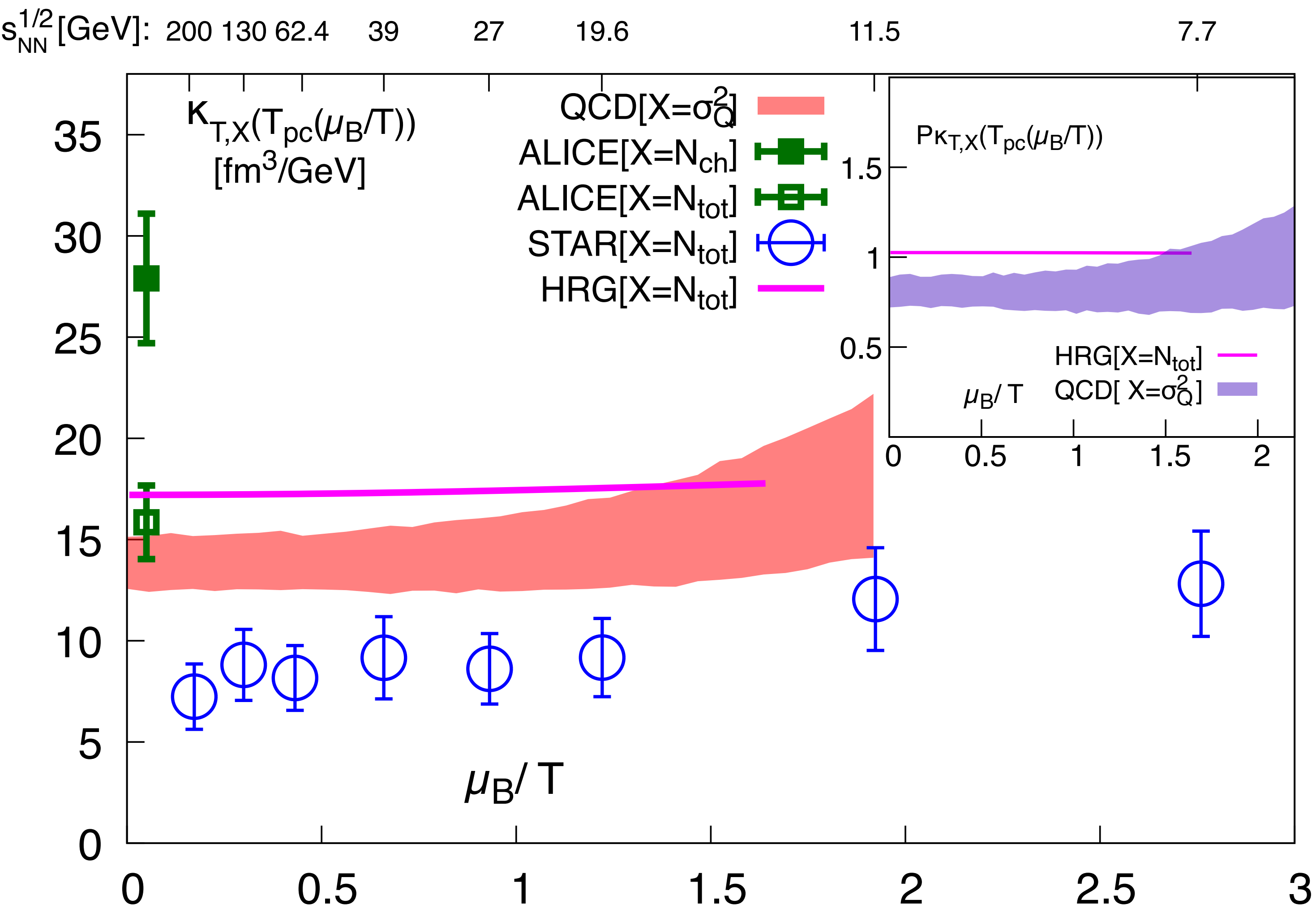

Rescaling the ALICE result by this HRG-based factor (1.8) brings it into reasonable agreement with the lattice-QCD result.

For STAR, we use the measured particle multiplicities together with HRG to estimate the corresponding scaled variance and κ_T .

In QCD both charged and neutral hadrons N_i contribute to the κ_T; For fixed particle number κ_T is,

$$\kappa^{-1}_{T,\vec{N}} = T^4 \sum_{i \in hadrons} \frac{\hat{n}_i}{\omega_i},\ \omega_i = \frac{\sigma_i^2}{N_i},$$

scaled variance.

ALICE results obtained only from charge particles; **Needs to be corrected for neutral particle contribution.**

In HRG, fixing the **total particle number yields an isothermal compressibility about 1.8 times smaller than fixing the charged-particle number** alone.

Stanislaw Mrowczynski, Phys.Lett. B430 (1998) 9-14;
ALICE, Eur. Phys. J. C 81 (2021) 1012;

Summary

CRC-TR 211

- Finite-density lattice QCD provides the EoS of strangeness-neutral matter in the BES-relevant range through Taylor expansion in μ_B/T .
- The same Taylor coefficients connect the three regimes: HRG at low T, crossover physics near T_{pc}, and perturbative behavior in the high-T. Thermal derivatives of P_2 and P_4 provides an estimate of the crossover temperature.
- From the same EoS we determine material response functions including, c_s^2, c_T^2 and c_V/T^3. Finite-density effects are largest below and around the crossover.
- A key new ingredient is a generalized QCD definition of the isothermal compressibility, using conserved-charge fluctuations rather than a fixed total particle number:
- Within the controlled Taylor range, the response observables show smooth crossover behavior, with no obvious critical enhancement. This is not an exclusion of a CEP.

Thank you for your attention!!

Energy and entropy density at finite chemical potentials

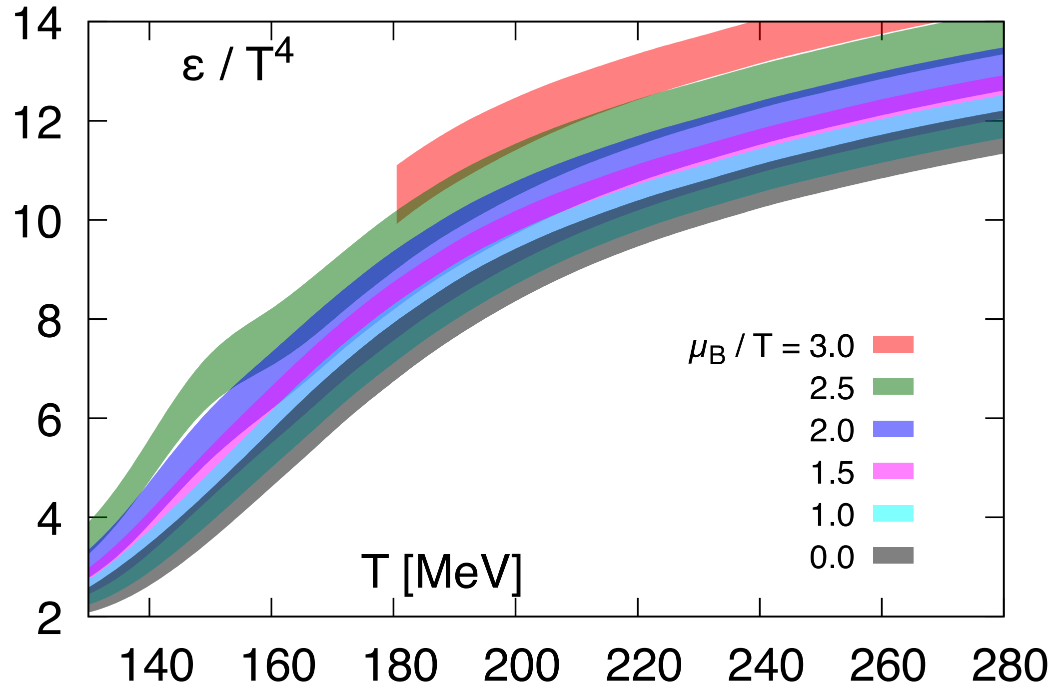

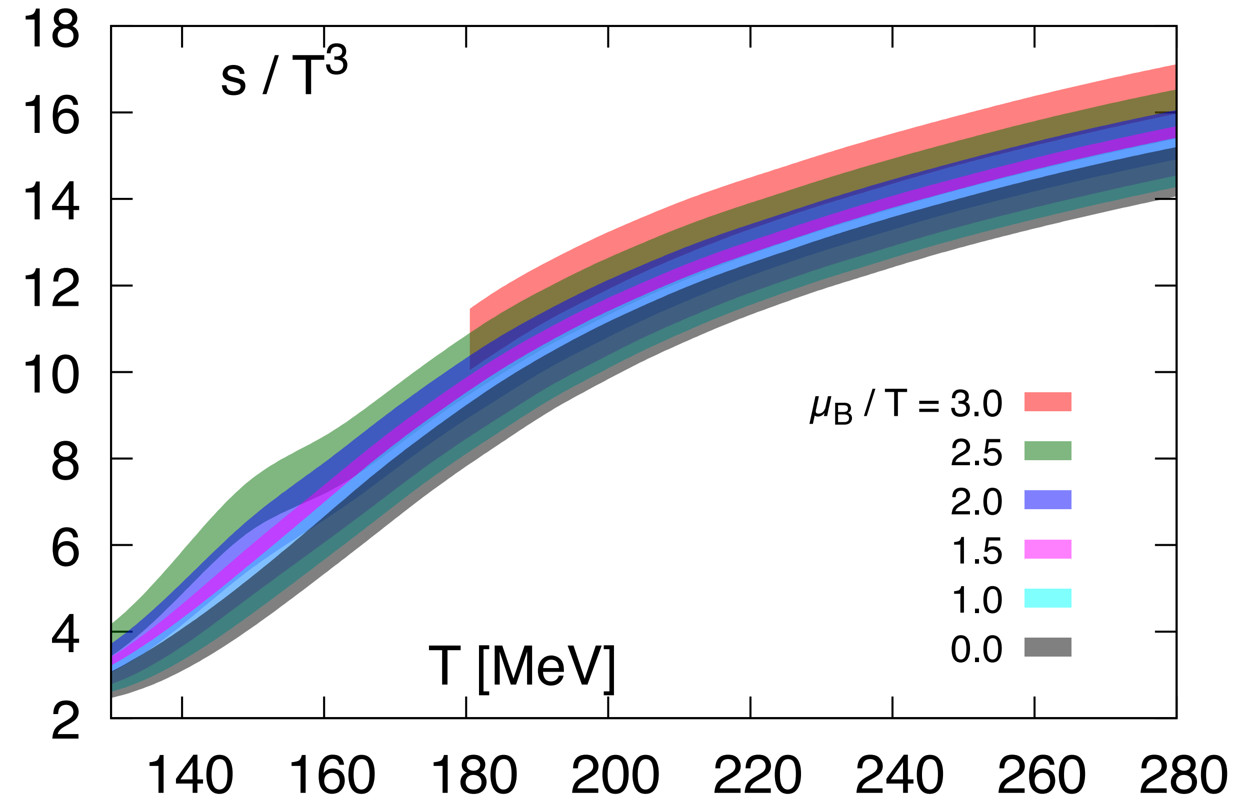

- $\hat{\mu}_B \equiv \frac{\mu_B}{T}, \qquad t = \frac{1}{t_0}\left[\frac{T-T_c}{T_c} + \kappa_2^B \hat{\mu}_B^2 + \cdots\right],$
  $\frac{\partial}{\partial \hat{\mu}_B^2} \sim \frac{\kappa_2^B}{t_0}\frac{\partial}{\partial t}, P_2^{\prime s} = T\frac{dP_2^s}{dT} \propto \kappa_2^B f_f''(z), P_4^s \propto (\kappa_2^B)^2 f_f''(z)$
- P_2' and P_4, share the same singular scaling function.
-

Toolbox

- Numbered list
  1. first item
  2. second item
  3. …

footnote or citation